

Electronic Supplementary Information

Phenethylammonium bismuth halides: from single crystals to bulky-organic cation promoted thin-film deposition for potential optoelectronic applications

Mehri Ghasemi ^a, Miaoqiang Lyu ^{*a}, Md Roknuzzaman ^b, Jung-Ho Yun ^a, Mengmeng Hao ^a, Dongxu He ^a, Yang Bai ^a, Peng Chen ^a, Paul V. Bernhardt ^c, Kostya (Ken) Ostrikov ^b and Lianzhou Wang^{*a}

^aNanomaterials Centre, School of Chemical Engineering and Australian Institute for Bioengineering and Nanotechnology, The University of Queensland, Brisbane, QLD, 4072, Australia. miaoqiang.lyu@gmail.com and l.wang@uq.edu.au

^bSchool of Chemistry, Physics and Mechanical Engineering and Institute of Future Environments, Queensland University of Technology (QUT), QLD 4000, Australia.

^cSchool of Chemistry and Molecular Biosciences, The University of Queensland, Brisbane, QLD, 4072, Australia

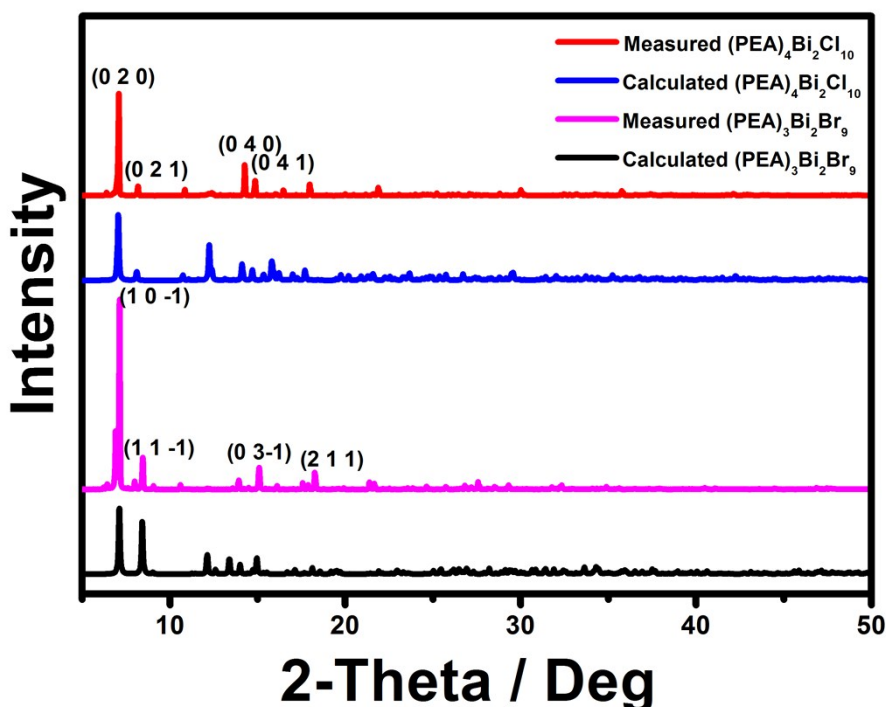


Figure S1. Calculated XRD pattern form single crystal characterization and powder XRD pattern of $(\text{PEA})_3\text{Bi}_2\text{Br}_9$ and $(\text{PEA})_4\text{Bi}_2\text{Cl}_{10}$.

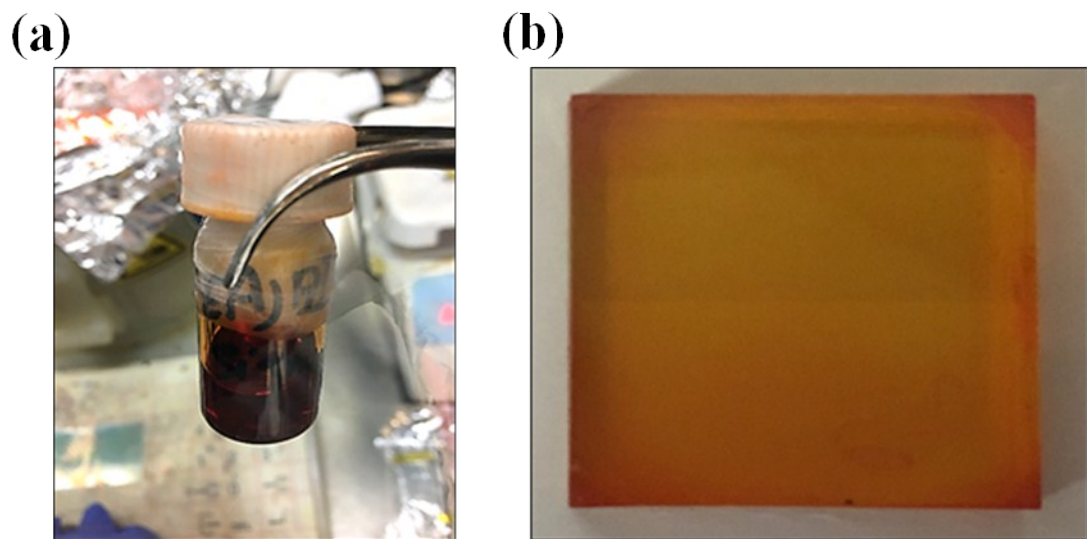


Figure S2. Red colour of the $(\text{PEA})_3\text{Bi}_2\text{I}_9$ (a) the primary solution and (b) film deposited on FTO .

Table S1. Crystal data and structure refinement for (PEA)₃Bi₂I₉, (PEA)₃Bi₂Br₉ and (PEA)₄Bi₂Cl₁₀

	(PEA) ₃ Bi ₂ I ₉	(PEA) ₃ Bi ₂ Br ₉	(PEA) ₄ Bi ₂ Cl ₁₀
Empirical formula	C ₂₄ H ₃₆ Bi ₂ I ₉ N ₃	C ₂₄ H ₃₆ Bi ₂ Br ₉ N ₃	C ₃₂ H ₄₈ Bi ₂ Cl ₁₀ N ₄
Formula weight	1926.62	1503.71	1261.20
Temperature	190(2) K	190(2) K	190(2) K
Wavelength	0.71073 Å	1.54184 Å	1.54184 Å
Crystal system	Monoclinic	Monoclinic	Monoclinic
Space group	P2 ₁ /n	P2 ₁ /n	P2 ₁ /c
Unit cell dimensions	a=14.5891(4) Å α = 90°	a=14.0039(2) Å α = 90°	a=7.9840(3) Å α = 90°
	b=20.4834(4) Å β = 113.030(3)°	b=19.5707(2) Å β = 115.492(2)°	b=25.0632(7) Å β = 91.161(3)°
	c=15.7858(4) Å γ = 90°	c=15.5528(3) Å γ = 90°	c=21.8464(6) Å γ = 90°
Volume	4341.37(18) Å ³	3847.52(10) Å ³	4370.7(2) Å ³
Z	4	4	4
Density (calculated)	2.948 Mg/m ³	2.596 Mg/m ³	1.917 Mg/m ³
Absorption coefficient	14.514 mm ⁻¹	28.850 mm ⁻¹	21.470 mm ⁻¹
F(000)	3376	2728	2416
Crystal size	3.35 to 25.00°	0.635 x 0.089 x 0.064 mm ³	0.1 x 0.05 x 0.01 mm ³
Theta range for data collection	3.35 to 25.00°.	3.56 to 62.44°.	4.05 to 62.49°.
Index ranges	-17<=h<=17, -24<=k<=24, -18<=l<=14	-16<=h<=16, -19<=k<=22, -17<=l<=17	-9<=h<=8, -28<=k<=28, -25<=l<=24
Reflections collected	21493	19929	23916
Independent reflections	7631 [R(int) = 0.0435]	6111 [R(int) = 0.0473]	6951 [R(int) = 0.0522]
Completeness to theta = 25.00°	99.7 %	99.7 %	99.7 %
Absorption correction	Semi-empirical from equivalents	Analytical	Semi-empirical from equivalents
Max. and min. transmission	1 and 0.2408	0.259 and 0.013	1 and 0.47589
Refinement method	Full-matrix least-squares on F ²	Full-matrix least-squares on F ²	Full-matrix least-squares on F ²
Data / restraints / parameters	7631 / 0 / 346	6111 / 0 / 346	6951 / 30 / 429
Goodness-of-fit on F²	1.020	1.136	1.018
Final R indices [I>2sigma(I)]	R1 = 0.0340, wR2 = 0.0639	R1 = 0.0375, wR2 = 0.1088	R1 = 0.0332, wR2 = 0.0722

R indices (all data)	R1 = 0.0463, wR2 = 0.0690	R1 = 0.0401, wR2 = 0.1111	R1 = 0.0442, wR2 = 0.0781
Largest diff. peak and hole	1.609 and -1.174 e. \AA^{-3}	1.301 and -2.042 e. \AA^{-3}	1.225 and -0.676 e. \AA^{-3}

Table S2. Atomic coordinates ($\times 10^4$) and equivalent isotropic displacement parameters ($\text{\AA}^2 \times 10^3$). U(eq)

is defined as one third of the trace of the orthogonalized U_{ij} tensor

		X	Y	Z	U(eq)
(PEA)₃Bi₂I₉	Bi(1)	-0.05359	0.42448	0.3244	0.026
	I(1)	-0.19295	0.08384	0.39218	0.037
	I(2)	0.12164	0.07302	0.43655	0.034
	N(1)	-0.2191	0.2751	0.9782	0.064
	C(1)	0.0112	0.1812	0.9456	0.036
	N(2)	0.1120	0.3957	0.6327	0.036
	C(2)	-0.0067	0.1188	0.9789	0.060
	C(3)	0.07910	0.08360	1.00780	0.068
(PEA)₃Bi₂Br₉	Bi(1)	0.05771	0.14810	0.66693	0.028
	Br(1)	-0.11709	0.07626	0.55840	0.036
	Br(2)	0.12096	0.06589	0.82055	0.043
	N(1)	-0.28250	0.22500	0.50200	0.049
	C(1)	-0.50070	0.32430	0.53540	0.042
	N(2)	0.34830	0.41640	0.82630	0.040
	C(2)	-0.58530	0.29790	0.54800	0.047
	Bi(1)	0.23481	0.52077	0.65285	0.034
(PEA)₄Bi₂Cl₁₀	Cl(1)	0.50890	0.55481	0.58921	0.064
	Cl(2)	0.20930	0.44601	0.57408	0.059
	N(1)	0.76140	0.59970	0.69710	0.074
	C(1)	0.86990	0.74800	0.70230	0.051
	N(2)	0.21100	0.96200	0.94830	0.028
	C(2)	0.78880	0.78560	0.66730	0.050

Table S3. Bond lengths [\AA] and angles [$^\circ$] for (PEA)₃Bi₂I₉, (PEA)₃Bi₂Br₉ and (PEA)₄Bi₂Cl₁₀.

(PEA)₃Bi₂I₉	Bond	Angle ($^\circ$)
	Bi(1)-I(1)	2.9446(6)
	Bi(1)-I(2)	2.9060(6)
	N(1)-C(8)	1.451(11)
	N(2)-C(16)	1.493(9)
	N(3)-C(24)	1.497(9)
(PEA)₃Bi₂Br₉	Bi(1)-Br(1)	2.6948(8)
	Bi(1)-Br(2)	2.6944(9)
	N(1)-C(8)	1.475(12)
	N(2)-C(16)	1.492(11)
	N(3)-C(24)	1.495(10)
(PEA)₄Bi₂Cl₁₀	Bi(1)-Cl (1)	2.7518(19)
	Bi(1)-Cl (2)	2.5493(16)
	N(1)-C(8)	1.494(7)
	N(2)-C(16)	1.494(8)
	N(3)-C(24)	1.476(10)

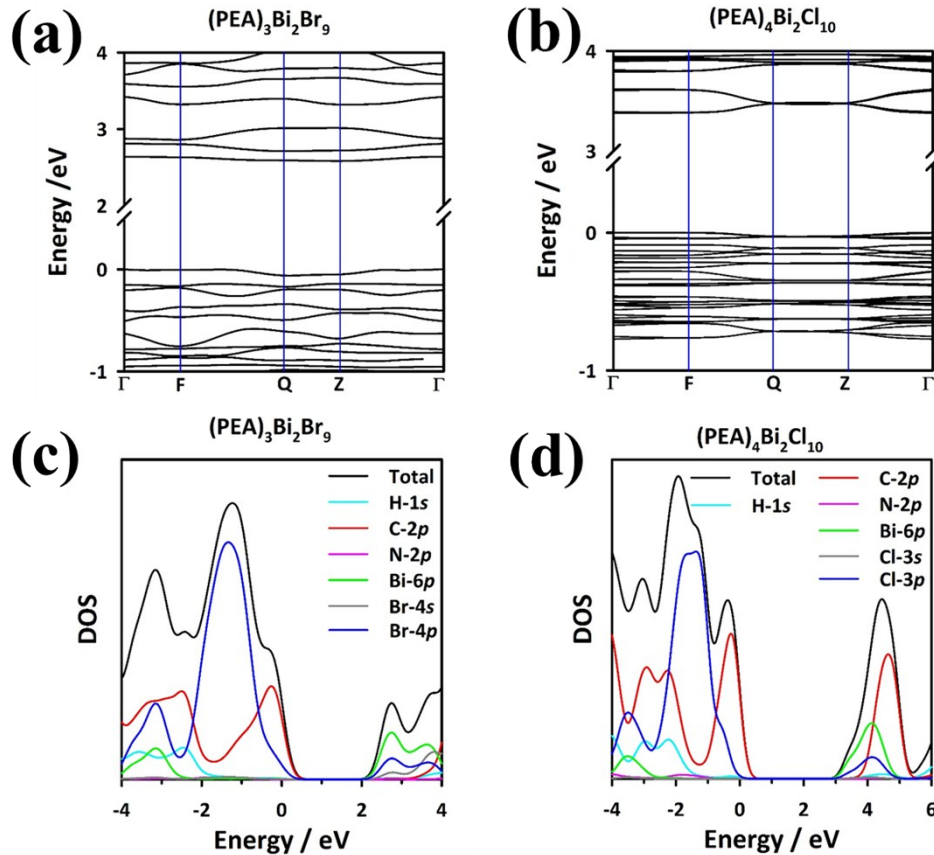


Figure S3. Calculated electronic band structures and total and partial densities of states (DOS) using Density Functional Theory (DFT) calculations (a) Band structure of $(\text{PEA})_3\text{Bi}_2\text{Br}_9$, (b) Band structure of $(\text{PEA})_4\text{Bi}_2\text{Cl}_{10}$, DOS of (c) $(\text{PEA})_3\text{Bi}_2\text{Br}_9$, (d) DOS of $(\text{PEA})_4\text{Bi}_2\text{Cl}_{10}$.

Table S4. Calculated direct band gap at different point of the Brillouin zone and minimum direct and indirect band gap, E_g (eV) of the considered compounds of $(\text{PEA})_3\text{Bi}_2\text{Br}_9$ and $(\text{PEA})_4\text{Bi}_2\text{Cl}_{10}$.

Compounds	Direct				Indirect	
	Γ (0, 0, 0)	F (0, 0.5, 0)	Q (0, 0.5, 0.5)	Z (0, 0, 0.5)	Minimum	
$(\text{PEA})_3\text{Bi}_2\text{Br}_9$	2.64	2.64	2.65	2.63	2.63	2.58
$(\text{PEA})_4\text{Bi}_2\text{Cl}_{10}$	3.37	3.38	3.5	3.49	3.37	3.33

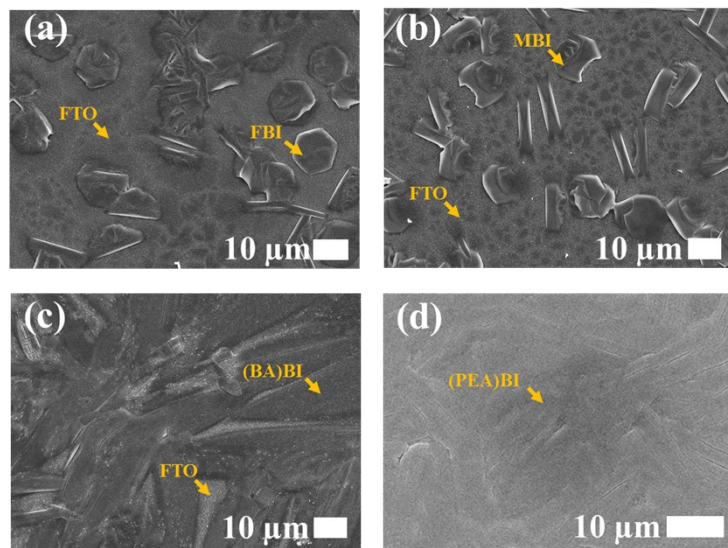


Figure S4. SEM images of $\text{A}_3\text{Bi}_2\text{I}_9$ film deposited on FTO with different organic cations of (a) Formamidium (CH_5N_2 , FA), (b) Methylammonium (CH_6N , MA), (c) n-Butylammonium ($\text{C}_4\text{H}_{12}\text{N}$, BA), (d) Phenethylammonium ($\text{C}_8\text{H}_{12}\text{N}$, PEA).

Table S5. Various device parameters of the best-performing devices with $\text{MA}_3\text{Bi}_2\text{I}_9$ and $(\text{PEA})_3\text{Bi}_2\text{I}_9$ as the active layer in FTO / C-TiO₂ / Perovskite derivative / P3HT / Au structure.

Active Layer	J_{sc} (mA/cm ²)	V_{oc} (V)	FF	PCE (%)
$\text{MA}_3\text{Bi}_2\text{I}_9$	0.24	0.43	0.42	0.043
$(\text{PEA})_3\text{Bi}_2\text{I}_9$	0.39	0.49	0.45	0.086

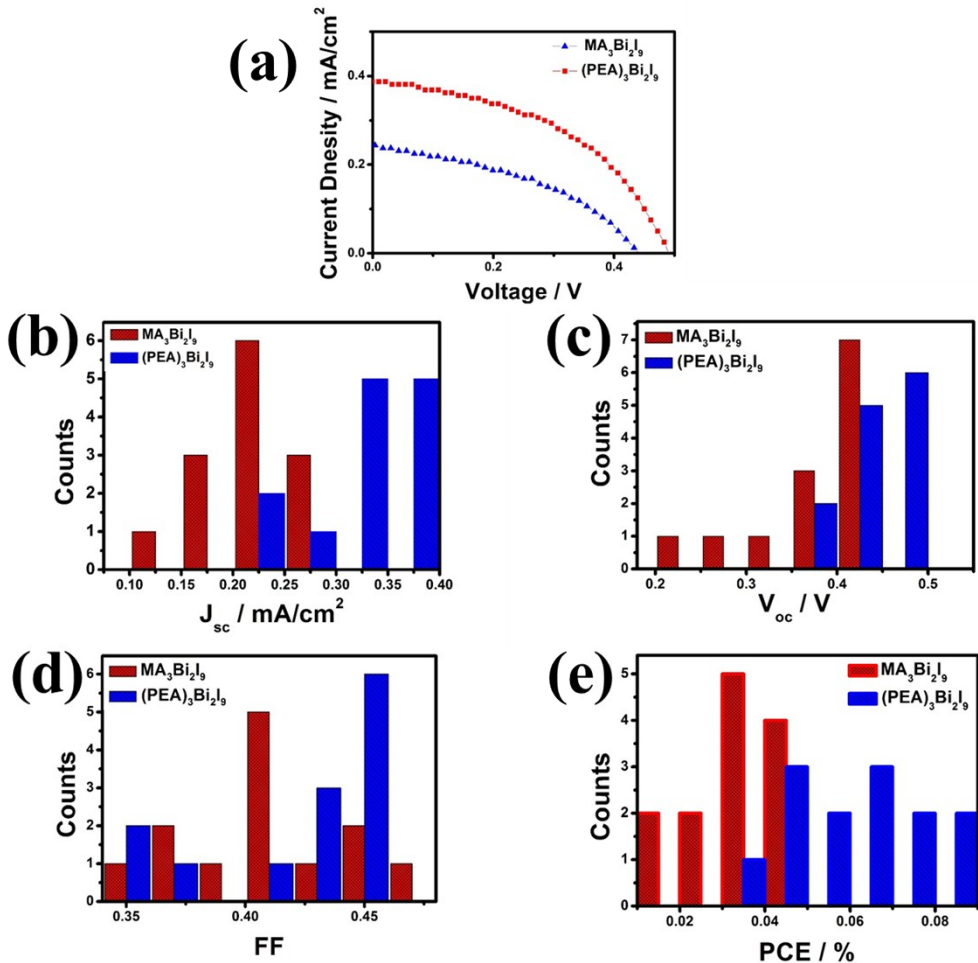


Figure S5. (a) J–V curve of the best performing devices with $\text{MA}_3\text{Bi}_2\text{I}_9$ and $(\text{PEA})_3\text{Bi}_2\text{I}_9$ as the active layer with FTO / C-TiO₂ / Perovskite derivative / P3HT/Au structure. Statistical photovoltaic parameters of 13 devices with FTO / C-TiO₂ / bismuth organohalides / P3HT/ Au structure, (b) J_{sc} , (c) V_{oc} , (d) FF, and (e) PCE.

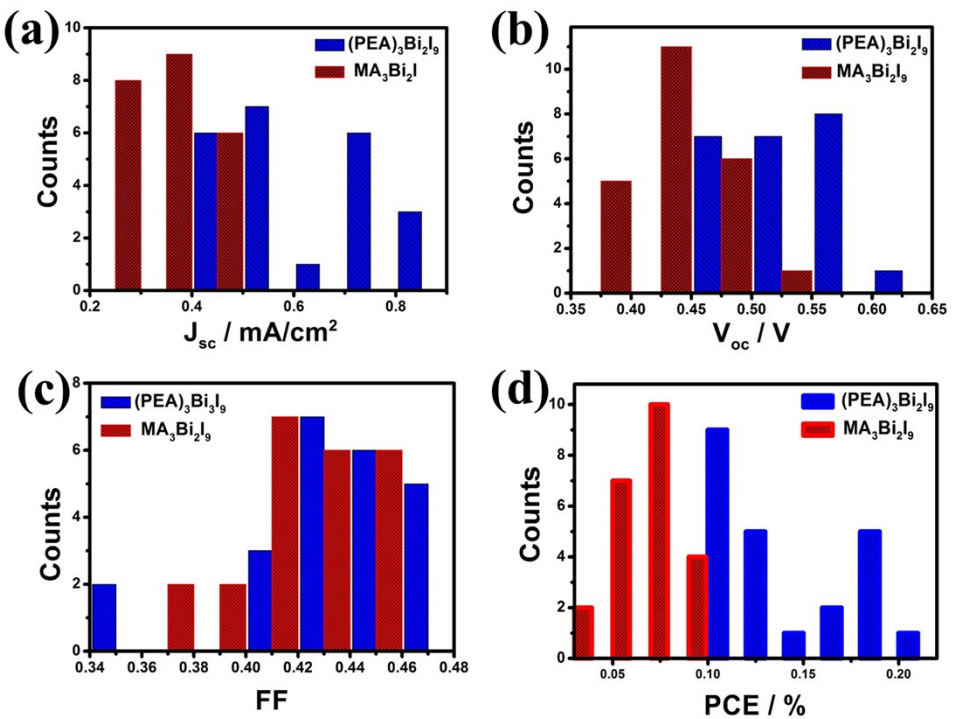


Figure S6. Statistical distribution of (a) J_{sc} , (b) V_{oc} , (c) FF and (d) PCE for 24 devices based on the $\text{MA}_3\text{Bi}_2\text{I}_9$ and $(\text{PEA})_3\text{Bi}_2\text{I}_9$ with FTO / C-TiO₂ / M-TiO₂ / bismuth organohalides / P3HT / Au structure.

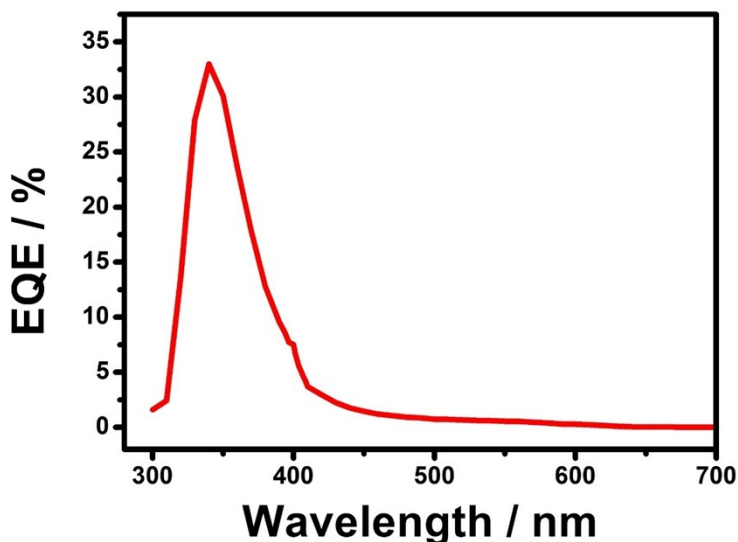


Figure S7. EQE results for the device with FTO / C-TiO₂ / M-TiO₂ / (PEA)₃Bi₂I₉ / P3HT / Au structure.

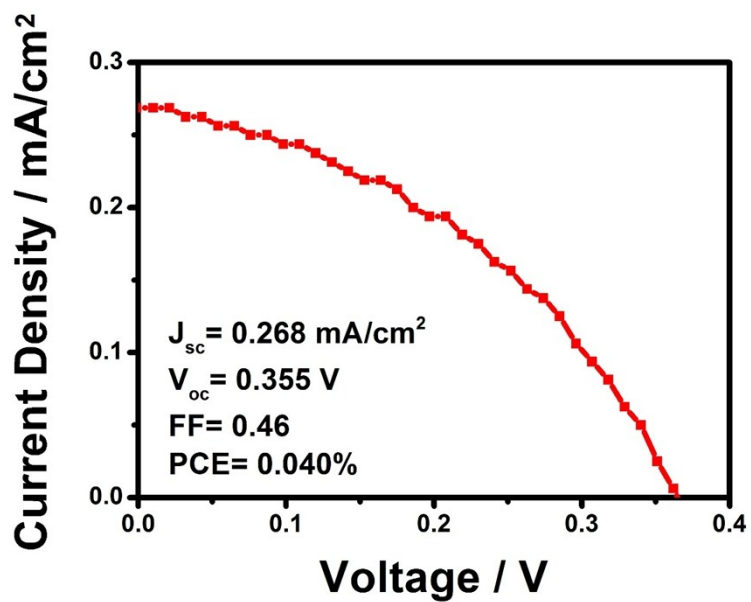


Figure S8. J–V curve of the device with the structure of FTO / C-TiO₂ / M-TiO₂ / P3HT / Au.

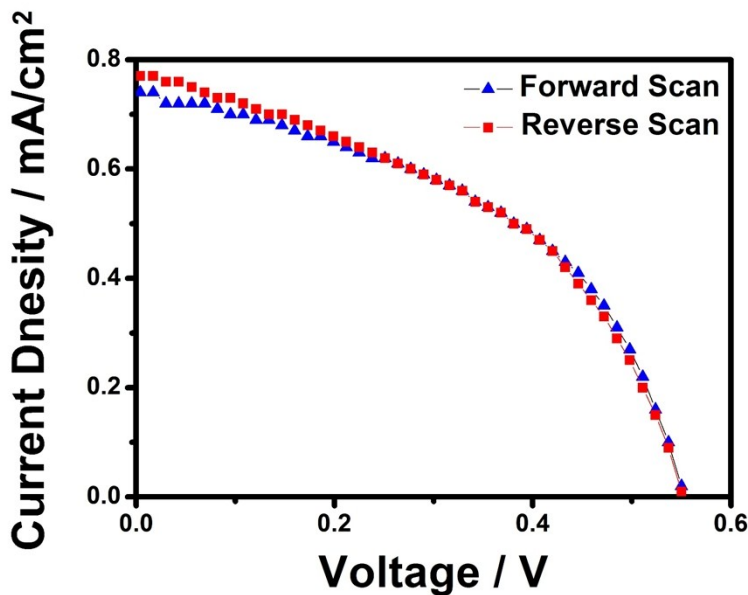


Figure S9. J–V curves of a (PEA)₃Bi₂I₉ device scanned from forward and reverse bias.

Table S6. Photovoltaic properties of (PEA)₃Bi₂I₉ based solar cell with various durations of storage in ambient air.

Time	J _{sc} (mA/cm ²)	V _{oc} (V)	FF	PCE (%)
Day 1	0.521	0.552	0.459	0.131
Day 4	0.812	0.557	0.46	0.183
Day 8	0.834	0.556	0.469	0.193
Day 10	0.814	0.590	0.45	0.216
Day 15	0.770	0.560	0.442	0.191
Day 20	0.740	0.559	0.436	0.18

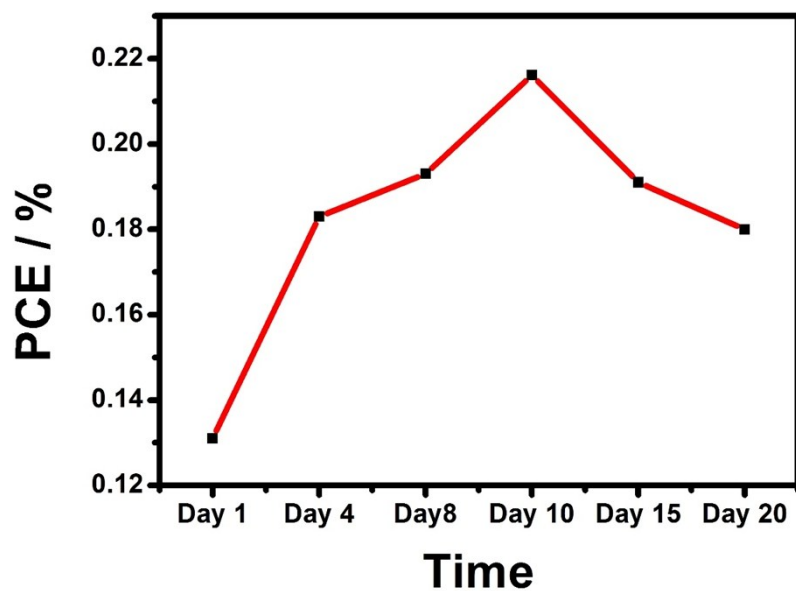


Figure S10. Efficiency of the $(\text{PEA})_3\text{Bi}_2\text{I}_9$ device with the structure of FTO / C-TiO₂ / M-TiO₂ / $(\text{PEA})_3\text{Bi}_2\text{I}_9$ / Au upon storage in air for 20 days.